Longitudinal Stability of a Hovering, Tethered Rotorcraft

D.C. Rye*
The University of Sydney, Sydney, Australia

Linearized equations describing the perturbed longitudinal motion of a tethered rotorcraft are presented. The tethering cable is assumed to be straight and inextensible. This permits development of two degree-of-freedom equations which admit cable tension variations. Routh's criteria are applied to a simplified stability quartic for hovering flight in an analytic search for stable configurations. The cable length, equilibrium tension, and point of attachment strongly influence the stability of perturbed motion. If the cable is short, the machines considered may be inherently stable. This does not appear to be possible for hovering flight on very long cables. Numerical solutions to the complete stability quartic show good agreement with approximate Routh's-criteria predictions.

Nomenclature†

A = area (m^2)
a = aerofoil lift curve slope (rad^{-1})
B = blade flapping moment of inertia ($kg\text{-}m^2$)
C_l, C_d = tailplane lift and drag coefficients
c_{11}, c_{12}, etc. = damping terms in the equation of motion
f_c = $F_c/\rho s A_r \Omega^2 R^2$ = dimensionless cable force
$\hat{g}$ = $g/\Omega^2 R$ = dimensionless acceleration due to gravity
h_c = $H/\rho s A_r \Omega^2 R^2$ = rotor H-force coefficient
I = vehicle moment of inertia in pitch ($kg\text{-}m^2$)
k = $\sqrt{I/mR^2}$ = dimensionless radius of gyration in pitch
k_{11}, k_{12}, etc. = stiffness terms in equation of motion
M = a pitching moment (N-m)
M_u, M_w, M_q, M_θ = pitching moment derivatives
$\hat{m}$ = $m/\rho s A_r R$ = dimensionless vehicle mass
m_u, m_w, m_q, m_θ = dimensionless pitching moment derivatives
m_{11}, m_{12}, etc. = inertia terms in the equation of motion
$\hat{q}$ = q/Ω = dimensionless pitch rate perturbation
R = rotor radius (m)
s = rotor solidity
t = time (s)
t_c = $T/\rho s A_r \Omega^2 R^2$ = Rotor thrust coefficient
U_0 = wind velocity ($m\text{-}s^{-1}$)
u = velocity perturbation in x-direction ($m\text{-}s^{-1}$)
$\hat{u}$ = $u/\Omega R$ = dimensionless x-velocity pertubation
v_{i0} = average induced velocity at the rotor ($m\text{-}s^{-1}$)
w = velocity perturbation in z-direction ($m\text{-}s^{-1}$)
$\hat{w}$ = $w/\Omega R$ = dimensionless z-velocity perturbation
X = force component in x-direction (N)
X_u, X_w, X_q, X_θ = X-force derivatives
x_u, x_w, x_q, x_θ = dimensionless x-force derivatives
Z = force component in z-direction (N)
Z_u, Z_w, Z_q, Z_θ = Z-force derivatives
z_u, z_w, z_q, z_θ = dimensioness z-force derivatives
α_c = cable angle (rad)
α_r = angle of relative wind at tailplane (rad)
Γ = $t_{ce}/\hat{m}\hat{g} = T/mg$ = thrust to weight ratio
ϵ = $1/\ell_c$
$\epsilon_0, \epsilon_1, \epsilon_2$ = coefficients in Fourier series for C_d
ζ = tailplane setting angle (rad)
θ = vehicle pitch attitude (rad)
θ_0 = blade collective pitch angle (rad)
ρ = air density ($kg\text{-}m^{-3}$)
τ = $t\Omega/\hat{m}$ = unit of dimensionless time
Ω = blade rotational speed ($rad\text{-}s^{-1}$)

Subscripts and Superscripts

Δ = perturbation from equilibrium
$\hat{(\ )}$ = dimensionless quantity
$(\ )^*$ = critical value of a quantity
$\dot{(\ )}$ = differentation with respect to t
$(\ )'$ = differentation with respect to τ
$(\ )_e$ = equilibrium quantity
$(\ )_p$ = association with the cable attachment point
$(\ )_r$ = association with the rotor
$(\ )_t$ = association with the tailplane

All rotor forces are referred to the axis of no feathering (ANF). As no cyclic pitch is applied, the ANF coincides with the shaft axis.

Introduction

APPLICATIONS involving the tethering of rotary winged aircraft have been proposed over many years. Recently, a resurgence of interest in these devices has emerged. Tethered helicopters find application where it is desirable to provide an elevated platform, stabilized in some operating orientation. These elevated platforms were applied originally to military tasks such as providing forward observation posts. As early as 1933,[2] the German company AEG experimented with an electrically powered tethered helicopter. More recently, McNeill et al.[3] have published a design study of such systems. Their report also summarizes some earlier work on tethered helicopters.

Recently, it has been suggested[4-7] that tropospheric winds might be used for electricity generation. The drag resulting is reacted by one or more tethers, through which electrical power and control signals may be transmitted. Unmanned rotary winged machines,[6,7] operating autorotatively, have been ad-

Received Nov. 30, 1983; revision received Feb. 6, 1985.

*Postgraduate Research Student, Department of Mechanical Engineering.

†The nomenclature adopted here generally follows that used by Bramwell.[1] Many of the variables are defined in Fig. 2; quantities have positive signs as depicted in the figure.

vanced as a practical way of simultaneously providing lift and extracting energy from the wind. The rotorcraft proposed, termed gyromill and gyroturbine, would operate in two basic modes: electrically powered hovering flight or windmilling power generation. When operating in wind, the machine's pitch attitude is controlled by a horizontal tailplane or tailrotor of suitable size. This enables the rotor to autorotate or to windmill at an incidence appropriate to the windspeed. The electrical loading of the rotor can be adjusted to maintain constant rotor speed. When the windspeed decreases below that required to provide lift in autorotation, the machine reverts to the powered mode. In this configuration, altitude may be maintained, or the device lowered to the ground.

Although the present analysis is applicable to other rotorcraft, it is primarily concerned with the device known as a gyromill. This machine, shown in Fig. 1, consists essentially of two counterrotating single bladed rotors coupled to electrical machines. The rotors are separated by a transverse fuselage and operate at constant speed in all modes. A longitudinal boom supports an all-moving fin and tailplane. Further construction details and preliminary experiments conducted with a research machine are reported by Blackler et al.[8]

The tethering of a lifting device profoundly affects its stability and response characteristics. Due to the interaction between the machine and its tether, the cable tension can be of the same magnitude as the vehicle aerodynamic forces. This is especially true during high disk incidence autorotative operation of the gyromill. As the vehicle translates, the geometrical constraint of the cable couples linear and angular motions, and so applies additional forces and moments to the craft. Despite the remarkably different characteristics attributable to the influence of the tether, few investigations of these effects are reported in the literature. For autorotative or windmilling operation, there appears to be no published work.

Historically, workers in the field of rotorcraft dynamics have chosen to adopt simplified cable models in their studies of tethered helicopter stability. Kaufman and Schultz[9] investigated the dynamics of a tethered synchropter using linearized equations of motion which involved the assumption of a straight cable under constant tension. By assuming zero damping, two principal modes were identified: a short period "pitching" mode and a nonoscillatory divergent "pendular" mode. Comments regarding the nature of the automatic control problem were also made. Simplified dynamic models were produced by Schmidt and Swik[10] by separation of the degrees of freedom and subsequent linearization. Various control strategies were applied to these models, and the results were compared with flight observations using appropriate automatic hover control hardware. Good correspondence between the model dynamics and the real system behavior was reported. With the cable attached below the center of gravity, the system displayed aperiodic instability. Using a simple tether model and neglecting the rotor dynamics, the nonlinear equations of motion were numerically integrated[11] to demonstrate that the "pendular" mode may be divergent or nondivergent, depending on the point of cable attachment. Variations in cable tension were found to be significant, particularly at short cable lengths. These two aspects are germane to any dynamic analysis of tethered rotorcraft.

Although there are few published investigations of tethered helicopter stability, many writers have addressed the problem of the stability of a cable towed or tethered body. Almost invariably, the body chosen is a heavy sphere; the investigation is then essentially one of cable dynamics. Glauert, in his seminal analysis[12] adopted a quasistatic approach to the cable dynamics by assuming the disturbed cable shape to depend only on the displacement of the towed body. He found that increasing the length of the body or the cable, or the drag of the body had a beneficial effect on stability. More recently, Huffman and Genin[13] included the effects of cable mass and elasticity in their study of the dynamics of a cable towing a heavy sphere. They believed the sole mechanism for instability to be a coupled resonance between the natural modes of the towed vehicle and those of the cable. Also of interest is Phillips' investigation[14] of the conditions necessary for aerodynamic forces to amplify transverse waves propagating on a towing cable. His theory indicates that waves propagating upwind are always damped, while downwind traveling waves are slightly damped if the wave velocity exceeds the airspeed. Consequently, Phillips reasons that all waves will decay if the towed body drag exceeds a certain small value. DeLaurier[15] has also contributed a thorough discourse on the stability of a body towed or tethered in a uniform free stream.

The current paper presents linearized equations describing the small perturbation behavior of a gyromill or similar rotorcraft when operating in wind, or simply hovering in still air.

Preliminary Assumptions

The equations describing the behavior of a tethered rotorcraft are complex, making analytic investigation of the stability or response difficult. Assumptions may be made which considerably reduce the complexity of the equations. The craft is assumed to behave as a rigid body and is taken to be symmetrical about the x-z plane. Due to the counterrotation of the rotors, longitudinal motion of the machine produces no resultant aerodynamic forces or moments in the lateral directions (y,ϕ,ψ). With these assumptions, and if the cable lies in the plane of symmetry when the motion starts, then the equations in six spatial degrees of freedom reduce to a consideration of uncoupled sets of "longitudinal" and "lateral" equations. Additionally, it is assumed that the fuselage aerodynamic forces are negligible.

In perturbed flight, it is assumed that the velocity induced by the rotors is independant of the rotor accelerations. The effect of rotor induced velocity on the tailplane derivatives is included, as is the influence of downwash lag. No allowance is made for interactions between rotors, or for ground effects when the cable length is small.

Since the principal intention of this work is to investigate the influence of geometrical and operational parameters on the dynamic behavior of the vehicle, simplifying assumptions are made regarding the tether. If the tension developed by a tethering cable is large in comparison with both the cable aerodynamic and weight forces, the cable drape will be slight. In this condition, readily attained by short cables under moderate tension, it is reasonable to neglect the cable weight and aerodynamic forces. If the structural elasticity of the cable is also neglected, it then behaves as a straight, massless, inextensible member. Clearly, real cables will sometimes depart substantially from this ideal. Nevertheless, this first-order ap-

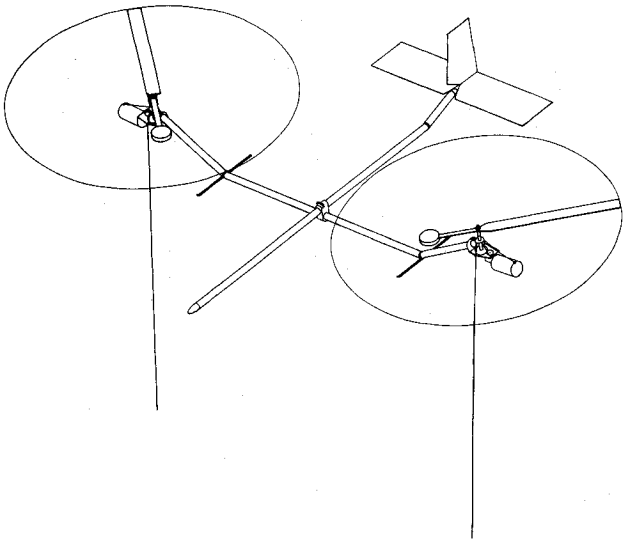

Fig. 1 Gyromill Mk.1 with twin 2.3 m diameter rotors.

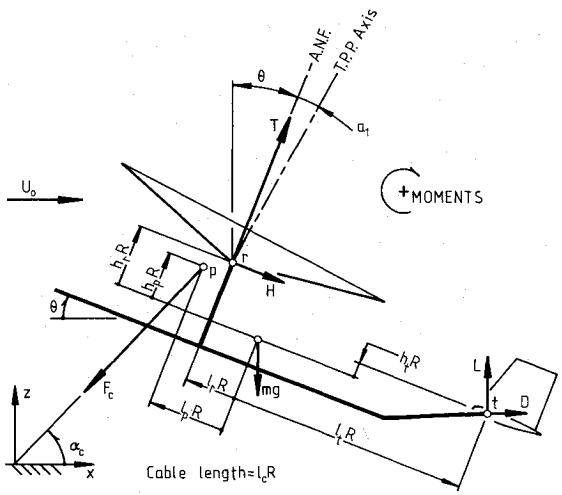

Fig. 2 Definition of machine geometry.

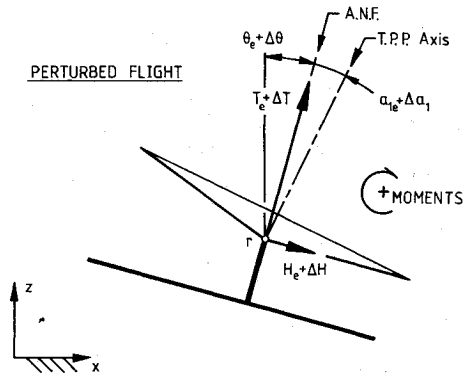

Fig. 3 Definition of rotor forces.

proximation is adopted in order to ascertain if an unstable craft may be stabilized by the action of a suitably located tethering cable. Kaufman and Schultz[10] admit this possibility but do not pursue the investigation.

Further motivation is provided by a report[2] that, in the early 1940's, an AEG electric helicopter made stable tethered flights to an altitude of 2,000 ft, apparently without artificial stabilization.

Longitudinal Equilibrium

Since one end of the cable is attached to the earth, it is convenient to define the machine's position with respect to earth-fixed axes, as shown in Fig. 2. If equilibrium is achieved without the application of cyclic pitch, then $\alpha_{nf}=\theta$. Using rotor forces referred to the ANF (shaft axis), the equations of equilibrium in the longitudinal plane are

$$-F_{ce}\cos\alpha_{ce}+T_e\sin\theta_e+H_e\cos\theta_e+D_e=0 \tag{1}$$

$$-F_{ce}\sin\alpha_{ce}+T_e\cos\theta_e-H_e\sin\theta_e+L_e-\mathrm{mg}=0 \tag{2}$$

$$-F_{ce}\ell_2R+T_e\ell_rR+H_eh_rR-L_e\ell_4R+D_eh_4R=0 \tag{3}$$

The quantities ℓ_2R, h_4R, etc. are various lengths and heights as defined in Appendix 1.

Solutions to the equilibrium equations are conveniently found by seeking the value of pitch attitude which yields zero pitching moment at the point of cable attachment. The equilibrium values of cable force and angle are then dictated solely by the requirement of force equilibrium. At values of T/mg near unity, the necessity for x-force equilibrium requires that small changes in pitch attitude lead to large excursions in cable angle. Consequently, if the cable is long, the machine will suffer large translations as the pitch attitude is varied.

Equations of Perturbed Motion

For small perturbations Δ from equilibrium, the vehicle equations of longitudinal motion may be expressed in the earth-fixed axes as

$$m\Delta\ddot{x}=-\Delta F_c\cos\alpha_{ce}+\Delta\alpha_cF_{ce}\sin\alpha_{ce}+\Delta X_r+\Delta X_t \tag{4}$$

$$m\Delta\ddot{z}=-\Delta F_c\sin\alpha_{ce}-\Delta\alpha_cF_{ce}\cos\alpha_{ce}+\Delta Z_r+\Delta Z_t \tag{5}$$

$$I\Delta\ddot{\theta}=-\Delta F_c\ell_2R-(\Delta\theta+\Delta\alpha_c)F_{ce}h_2R+\Delta M_r+\Delta M_t \tag{6}$$

where the force and moment contributions due to the rotor and tailplane are denoted by ΔX_r, ΔM_t etc.

Solutions to these three equations of motion must also satisfy the geometrical constraints imposed by the assumption of a straight, inextensible cable. In differential form, the constraint equations are

$$\Delta x=-\Delta\alpha_c\ell_cR\sin\alpha_{ce}-\Delta\theta h_1R \tag{7}$$

$$\Delta z=\Delta\alpha_c\ell_cR\cos\alpha_{ce}-\Delta\theta\ell_1R \tag{8}$$

Before proceeding with the vehicle equations of motion, it is necessary to express the perturbations in rotor and tailplane force and moment in terms of the dependent variables Δx, Δz and $\Delta\theta$, and the control variables $\Delta\theta_0$ and $\Delta\zeta$.

Rotor Derivatives

Expressions for the perturbation quantities ΔX_r, ΔZ_r and ΔM_r may readily be found by applying classical linearization methods. In the disturbed flight condition shown in Fig. 3, the vehicle center of gravity has perturbation velocities $u=\Delta\dot{x}$, $w=\Delta\dot{z}$ and $q=\Delta\dot{\theta}$, which give rise to perturbations of rotor forces. The usual linearization procedure permits the rotor force perturbation in the direction of the earth-fixed x axis to be expressed as

$$\begin{aligned}\Delta X_r&=\Delta\theta\left[T_e\cos\theta_e-H_e\sin\theta_e+\frac{\partial X_r}{\partial\theta}\right]+\frac{\partial X_r}{\partial u_r}\cdot u_r\\&+\frac{\partial X_r}{\partial w_r}\cdot w_r+\frac{\partial X_r}{\partial q}\cdot q+\frac{\partial X_r}{\partial\theta_0}\cdot\Delta\theta_0\\&=\Delta\theta(T_e\cos\theta_e-H_e\sin\theta_e+X_{\theta r})\\&+X_{ur}\cdot u_r+X_{wr}\cdot w_r+X_{qr}\cdot q+X_{\theta_0}\cdot\Delta\theta_0\end{aligned} \tag{9}$$

where

$$X_{ur}=\frac{\partial T}{\partial u_r}\sin\theta_e+\frac{\partial H}{\partial u_r}\cos\theta_e,\ \text{etc.}$$

Similarly, ΔZ_r may be expressed as

$$\begin{aligned}\Delta Z_r&=\Delta\theta(-T_e\sin\theta_e-H_e\cos\theta_e+Z_{\theta r})\\&+Z_{ur}\cdot u_r+Z_{wr}\cdot w_r+Z_{qr}\cdot q+Z_{\theta_0}\cdot\Delta\theta_0\end{aligned} \tag{10}$$

where

$$Z_{wr}=\frac{\partial T}{\partial w_r}\cos\theta_e-\frac{\partial H}{\partial w_r}\sin\theta_e,\ \text{etc.}$$

Assuming that the rotors have zero flapping hinge offset, the perturbation in pitching moment is due solely to the change in rotor force. This moment perturbation is then

$$\Delta M_r=M_{\theta r}\cdot\Delta\theta+M_{ur}\cdot u_r+M_{wr}\cdot w_r+M_{qr}\cdot q+M_{\theta_0}\cdot\Delta\theta_0 \tag{11}$$

where

$$M_{ur}=\frac{\partial T}{\partial u_r}\ell_r R+\frac{\partial H}{\partial u_r}h_r R, \text{ etc.}$$

The derivatives $X_{\theta r}$, $Z_{\theta r}$ and $M_{\theta r}$ represent changes in rotor force and moment due to changing rotor inflow with pitch incidence. They do not appear in the usual rotorcraft equations of motion derived in body-fixed axes but must be included here, where all equations are written in an earth-fixed frame. All derivatives with respect to θ vanish when the rotor is hovering in still air.

In the preceding expressions, u_r and w_r are velocities at the rotor hub, measured with respect to the earth axes. Due to the pitching motion, the rotor hub has additional velocity relative to the center of gravity. Upon discarding terms of second order in disturbance quantities, the rotor hub velocity components are

$$u_r=\Delta\dot{x}+\Delta\dot{\theta}h_3 R \tag{12}$$

$$w_r=\Delta\dot{z}+\Delta\dot{\theta}\ell_3 R \tag{13}$$

$$q=\Delta\dot{\theta} \tag{14}$$

These three relations, together with the Eqs. (9-11) give expressions for the perturbations in rotor force and moment in terms of the velocity perturbations of the vehicle's center of gravity.

It should be noted that the rotor aerodynamic derivatives, such as $\partial T/\partial u_r$, which appear in these expressions are not the usual helicopter derivatives formulated in body-fixed axes. In general, these moving axes are not aligned with the earth-fixed axes, so that care must be taken in transforming the conventional derivatives into the earth-fixed frame.

Tailplane Derivatives

In deriving expressions for the tailplane perturbation quantities ΔX_t, ΔZ_t and ΔM_t it is useful to seek expressions which are valid for a wide range of pitch incidence. Accordingly, it is assumed that the tailplane lift and drag coefficients may be represented by

$$C_l=a_t\sin\alpha_r;\quad C_d=\epsilon_0+\epsilon_1\sin\alpha_r+\epsilon_2\cos\alpha_r$$

This approach, first suggested by Castles and New,[16] yields coefficients identical to those calculated by the usual theory when α_r approaches zero. For large angles of attack, both theories give results at variance with experiment. The above laws are preferred, however, as their use does not require an assumption that the inflow angle $\phi=\alpha_r-(\theta+\zeta)$ is small.

Again, linearization permits the perturbations in tailplane force and moment to be expressed as

$$\Delta X_t=X_{ut}\cdot\Delta\dot{x}+X_{wt}\cdot\Delta\dot{z}+X_{qt}\cdot\Delta\dot{\theta}+X_{\theta t}\cdot\Delta\theta+X_\zeta\cdot\Delta\zeta \tag{15}$$

$$\Delta Z_t=Z_{ut}\cdot\Delta\dot{x}+Z_{wt}\cdot\Delta\dot{z}+Z_{qt}\cdot\Delta\dot{\theta}+Z_{\theta t}\cdot\Delta\theta+Z_\zeta\cdot\Delta\zeta \tag{16}$$

and

$$\Delta M_t=M_{\dot{u}t}\cdot\Delta\ddot{x}+M_{\dot{w}t}\cdot\Delta\ddot{z}+M_{\dot{q}t}\cdot\Delta\ddot{\theta}+M_{ut}\cdot\Delta\dot{x}+M_{wt}\cdot\Delta\dot{z}$$
$$+M_{qt}\cdot\Delta\dot{\theta}+M_{\theta t}\cdot\Delta\theta+M_\zeta\cdot\Delta\zeta \tag{17}$$

In Eqs. (15) and (16) the acceleration derivatives due to downwash lag have been discarded as small, although these terms could easily have been retained. Expressions for the various aerodynamic derivatives are presented in Appendix 2. These expressions include the effects of aerodynamic interaction between rotor and tailplane. Inspection shows that all tailplane derivatives are negligible when the machine is hovering in still air.

The Nondimensional Equations of Motion

Upon substitution of the Eqs. (9-17) into Eq. (4-6), the equations of motion may be written in a more explicit form. It is also convenient to transform the equations of motion to a dimensionless form. The particular nondimensionalisation scheme chosen follows that used by Bramwell.[1] Although this transformation does not appreciably alter the equations of motion, it is in accordance with conventional rotorcraft practice, and so facilitates evaluation of the rotor derivatives in their usual form. From this point, the Δ notation for perturbations will be discontinued. Taking the rotor force coefficients t_{ce} and h_{ce} and the rotor derivatives x_{ur}, z_{wr}, etc. to refer to the complete rotor set, the nondimensional equations of perturbed motion are

$$\frac{d\hat{u}}{d\tau}-\hat{u}\cdot x_u-\hat{w}\cdot x_w+f_c(\cos\alpha_{ce})-\alpha_c(f_{ce}\sin\alpha_{ce})$$
$$-\frac{d\theta}{d\tau}\frac{1}{\hat{m}}(h_3x_{ur}+\ell_3x_{wr}+x_q)$$
$$-\theta(t_{ce}\cos\theta_e-h_{ce}\sin\theta_e+x_\theta)=x_{\theta_0}\theta_0+x_\zeta\zeta \tag{18}$$

$$\frac{d\hat{w}}{d\tau}-\hat{u}\cdot z_u-\hat{w}\cdot z_w+f_c(\sin\alpha_{ce})+\alpha_c(f_{ce}\cos\alpha_{ce})$$
$$-\frac{d\theta}{d\tau}\frac{1}{\hat{m}}(h_3z_{ur}+\ell_3z_{wr}+z_q)$$
$$-\theta(-t_{ce}\sin\theta_e-h_{ce}\cos\theta_e+z_\theta)=z_{\theta_0}\theta_0+z_\zeta\zeta \tag{19}$$

$$-\frac{d\hat{u}}{d\tau}\cdot m'_{ut}-\hat{u}\cdot m_u-\frac{d\hat{w}}{d\tau}\cdot m'_{wt}-\hat{w}\cdot m_w$$
$$+f_c\cdot\ell_2+\alpha_c\cdot f_{ce}h_2+\frac{d^2\theta}{d\tau^2}\frac{1}{\hat{m}}(k^2-h_3m'_{ut}-\ell_3m'_{wt}-m'_{qt})$$
$$-\frac{d\theta}{d\tau}\frac{1}{\hat{m}}(h_3m_{ur}+\ell_3m_{wr}+m_q)$$
$$-\theta(-f_{ce}h_2+m_\theta)=m_{\theta_0}\theta_0+m_\zeta\zeta \tag{20}$$

where an unsubscripted aerodynamic derivative refers to the complete machine: for example, $x_u=(x_{ur}+x_{ut})$ etc.

The differential Eqs. (7) and (8), representing the constraints imposed by the cable, give expressions for $\hat{u}$ and $\hat{w}$ in terms of θ and α_c. These cable equations allow the elimination of $\hat{u}$ and $\hat{w}$, and permit the perturbation equations to be written as

$$-\ddot{\theta}\cdot h_1+\ddot{\theta}(h_1\cdot x_u+\ell_1\cdot x_w-h_3x_{ur}-\ell_3x_{wr}-x_q)$$
$$-\theta[\hat{m}(t_{ce}\cos\theta_e-h_{ce}sin\theta_e+x_\theta)]$$
$$-\ddot{\alpha}_c(\ell_c\sin\alpha_{ce})+\dot{\alpha}_c(\ell_c\sin\alpha_{ce}\cdot x_u-\ell_c\cos\alpha_{ce}\cdot x_w)$$
$$-\alpha_c(\hat{m}f_{ce}\sin\alpha_{ce})+f_c(\hat{m}\cos\alpha_{ce})=\hat{m}(x_{\theta_0}\theta_0+x_\zeta\zeta) \tag{21}$$

$$-\ddot{\theta}\cdot\ell_1+\dot{\theta}(h_1\cdot z_u+\ell_1\cdot z_w-h_3z_{ur}-\ell_3z_{wr}-z_q)$$
$$-\theta[\hat{m}(-t_{ce}\sin\theta_e-h_{ce}\cos\theta_e+z_\theta)]$$
$$+\ddot{\alpha}_c(\ell_c\cos\alpha_{ce})+\dot{\alpha}_c(\ell_c\sin\alpha_{ce}\cdot z_u-\ell_c\cos\alpha_{ce}\cdot z_w)$$
$$+\alpha_c(\hat{m}f_{ce}\cos\alpha_{ce})+f_c(\hat{m}\sin\alpha_{ce})=\hat{m}(z_{\theta_0}\theta_0+z_\zeta\zeta) \tag{22}$$

$$\ddot{\theta}[k^2+(h_1-h_3)m'_{ut}+(\ell_1-\ell_3)m'_{wt}-m'_{qt}]$$
$$+\dot{\theta}(h_1\cdot m_u+\ell_1\cdot m_w-h_3m_{ur}-\ell_3m_{wr}-m_q)$$
$$+\theta[\hat{m}(f_{ce}h_2-m_\theta)]+\ddot{\alpha}_c[\ell_c(m'_{ut}\sin\alpha_c-m'_{wt}\cos\alpha_c)]$$
$$+\dot{\alpha}_c(\ell_c\sin\alpha_{ce}\cdot m_u-\ell_c\cos\alpha_{ce}\cdot m_w)$$
$$+\alpha_c(\hat{m}f_{ce}h_2)+f_c(\hat{m}\ell_2)=\hat{m}(m_{\theta_0}\theta_0+m_\zeta\zeta) \quad (23)$$

After elimination of cable force terms, the dimensionless equations of motion [Eqs. (21-23)] may be seen to involve only the two degrees of freedom θ and α_c. Equation (23) provides an expression relating the cable force perturbation f_c to the variables θ and α_c, and to the control variables θ_0 and ζ. Substitution of this expression into the Eqs. (21) and (22) eliminates f_c. The resulting equations may conveniently be written in matrix form as

$$[m]\ddot{x}+[c]\dot{x}+\hat{m}[k]x=\hat{m}[f]u \quad (24)$$

where

$$x=\{\theta,\alpha_c\}^T, \qquad u=\{\theta_0,\zeta\}^T$$

In this equation, the matrix elements are

$$m_{11}=h_1\ell_2+[k^2+(h_1-h_3)m'_{ut}+(\ell_1-\ell_3)m'_{wt}-m'_{qt}]\cos\alpha_{ce}$$
$$m_{12}=\ell_c[\ell_2\sin\alpha_{ce}+(m'_{ut}\sin\alpha_{ce}+m'_{wt}\cos\alpha_{ce})\cos\alpha_{ce}]$$
$$m_{21}=\ell_1\ell_2+[k^2+(h_1-h_3)m'_{ut}+(\ell_1-\ell_3)m'_{wt}-m'_{qt}]\sin\alpha_{ce}$$
$$m_{22}=\ell_c[-\ell_2\cos\alpha_{ce}+(m'_{ut}\sin\alpha_{ce}-m'_{wt}\cos\alpha_{ce})\sin\alpha_{ce}]$$
$$c_{11}=-\ell_2(h_1\cdot x_u+\ell_1\cdot x_w-h_3x_{ur}-\ell_3x_{wr}-x_q)$$
$$+\cos\alpha_{ce}(h_1\cdot m_u+\ell_1\cdot m_w-h_3m_{ur}-\ell_3m_{wr}-m_q)$$
$$c_{12}=-\ell_c\ell_2(x_u\cdot\sin\alpha_{ce}-x_w\cdot\cos\alpha_{ce})$$
$$+\ell_c\cos\alpha_{ce}(m_u\cdot\sin\alpha_{ce}-m_w\cdot\cos\alpha_{ce})$$
$$c_{21}=-\ell_2(h_1\cdot z_u+\ell_1\cdot z_w-h_3z_{ur}-\ell_3z_{wr}-z_q)$$
$$+\sin\alpha_{ce}(h_1\cdot m_u+\ell_1\cdot m_w-h_3m_{ur}-\ell_3m_{wr}-m_q)$$
$$c_{22}=-\ell_c\ell_2(z_u\cdot\sin\alpha_{ce}-z_w\cdot\cos\alpha_{ce})$$
$$+\ell_c\sin\alpha_{ce}(m_u\cdot\sin\alpha_{ce}-m_w\cdot\cos\alpha_{ce})$$
$$k_{11}=\ell_2(t_{ce}\cos\theta_e-h_{ce}\sin\theta_e+x_\theta)+(h_2f_{ce}-m_\theta)\cos\alpha_{ce}$$
$$k_{12}=\ell_1f_{ce}$$
$$k_{21}=\ell_2(-t_{ce}\sin\theta_e-h_{ce}\cos\theta_e+z_\theta)+(h_2f_{ce}-m_\theta)\sin\alpha_{ce}$$
$$k_{22}=-h_1f_{ce}$$
$$f_{11}=-\ell_2x_{\theta_0}+m_{\theta_0}\cos\alpha_{ce}$$
$$f_{12}=-\ell_2x_\zeta+m_\zeta\cos\alpha_{ce}$$
$$f_{21}=-\ell_2z_{\theta_0}+m_{\theta_0}+\sin\alpha_{ce}$$
$$f_{22}=-\ell_2z_\zeta+m_\zeta\sin\alpha_{ce}$$

The quantity $\hat{m}$ arises as a consequence of the particular scaling adopted, and is usually termed the relative density parameter. These equations of perturbed motion are quite general, applying to tethered flight in powered, autorotative or windmilling states.

Preamble to the Stabilty Analysis

Despite previous investigations, it is not clear where the tethering cable should best be attached, or how the flight characteristics will be influenced by changes in rotor thrust, cable length, wind speed, or other operational parameters. Furthermore, the dynamic characteristics of a powered rotor are quite different from those of a rotor in autorotative or windmilling flight.

Setting the control functions θ_0 and ζ in Eq. (24) to zero, and assuming that solutions are of the form $e^{s\tau}$ leads to the characteristic equation

$$[m_{11}m_{22}-m_{12}m_{21}]s^4+[m_{11}c_{22}+m_{22}c_{11}-m_{12}c_{21}$$
$$-m_{21}c_{12}]s^3+[\hat{m}(m_{11}k_{22}+m_{22}k_{11}-m_{12}k_{21}$$
$$-m_{21}k_{12})+c_{11}c_{22}-c_{12}c_{21}]s^2$$
$$+\hat{m}[c_{11}k_{22}+c_{22}k_{11}-c_{12}k_{21}-c_{21}k_{12}]s$$
$$+\hat{m}^2[k_{11}k_{22}-k_{12}k_{21}]=0 \quad (25)$$

Here, $s=\sigma+j\omega$ is the Laplace variable. Although numerical solution of this characteristic equation is straightforward, further insight into the machine's behavior can be gained from the Routh-Hurwitz criteria. In the most general equilibrium condition, high disk-incidence flight in wind, such analytic determination of parameters characterizing the disturbed motion is difficult. This is due to the complexity of the Routh test functions. When the machine is hovering in still air, many rotor derivatives and all of the trailplane derivatives may be neglected. Further simplifications may be made for the special case of hovering flight at zero craft incidence. In this condition, the device is restrained by a vertical tether.

It is the writer's opinion that stable hovering flight is a more difficult objective than stable flight in wind. This is because the tailplane is unable to significantly contribute to the machine's stability in the absence of wind. The remainder of this analysis is therefore restricted to an examination of hovering flight in still air. In this mode, the stability derivatives consist entirely of contributions due to the rotors. Accordingly, the subscript r will be omitted from rotor derivatives for the remainder of the analysis

Stability with Zero Damping

Neglecting rotor and tailplane damping terms considerably reduces the complexity of the stability criteria. This simplification promotes insight into the dynamic behavior of the rotorcraft on its tether. With the assumption of zero damping, the general stability quartic [Eq. (25)] reduces to a quadratic in s^2. In the special case of hovering flight, this quadratic is simply

$$[\ell_c(k^2+\ell_p^2)]s^4+[\hat{m}f_{ce}(k^2+\ell_p^2+h_p^2-h_p\ell_c)]s^2$$
$$+\hat{m}^2f_{ce}h_p\hat{m}\hat{g}=0$$

As there is no dissipation of energy, this characteristic equation represents, at best, marginally stable motion. Routh gives special rules for this case, and Nissim[17] has developed determinental functions applicable to marginally stable systems. Accordingly, for marginal stability it is necessary and sufficient that

$$h_p>0 \quad (26)$$

$$\ell_c<\ell_c^*, \quad \text{where} \quad \ell_c^*=(k^2+\ell_p^2+h_p^2)/h_p \quad (27)$$

$$(\Gamma-1)>4\ell_c/h_p\cdot(k^2+\ell_p^2)/(\ell_c^*-\ell_c)^2 \quad (28)$$

Equation (27) defines a critical value of ℓ_c, namely ℓ_c^*. By substituting $n\ell_c^*$ for ℓ_c, Eq. (28) may be written as

$$(\Gamma-1)>\frac{4n}{(1-n)^2}\cdot\frac{(k^2+\ell_p^2)}{(k^2+\ell_p^2+h_p^2)}, \qquad 0<n<1 \tag{29}$$

Equations (26) and (29) specify the boundaries of marginal stability for this simplistic undamped case. Clearly, if instability is to be avoided for flight on long cables, then h_p should be chosen small and positive. Selection of h_p negative (tether attachment point lower than center of gravity) will result in a statically unstable system; any disturbance from equilibrium will precipitate a nonoscillatory divergent motion. Equation (29) defines a minimum thrust to weight ratio which becomes large as ℓ_c approaches ℓ_c^*.

Inclusion of Rotor Damping

The zero damping stability analysis is quite artificial; considerable rotor damping will always exist, even when hovering in still air. In general, the coefficients of the damping matrix of Eq. (24) will not be small. This is particularly so at longer cable lengths, since ℓ_c scales the damping coefficient in the α_c direction. With the inclusion of all rotor damping terms, the Routh test functions become intractable (although numerically soluble) even for the simple hovering case. For this case, however, only a small number of derivatives are dominant. Accordingly, a simple but more realistic stability prediction may be made by incorporating the rotor force derivatives x_u, z_w and x_q into the analysis. As the flapping hinge offset is assumed zero, the moment derivatives depend only on the force derivatives and machine geometry. For the special case of hovering flight where θ_e is zero and the cable is vertical, the stability quartic is

$$\begin{aligned}&\ell_c[k^2+\ell_p^2]s^4-\ell_c[(k^2+\ell_p^2+h_r^2)x_u+(\ell_p-\ell_r)^2z_w+h_rx_q]s^3\\&+[\hat{m}f_{ce}(k^2+\ell_p^2+h_p^2-h_p\ell_c)+\ell_c(\ell_p-\ell_r)^2z_wx_u]s^2\\&-\hat{m}\{f_{ce}[((h_r-h_p)^2+\ell_c(h_r-h_p))x_u+(\ell_p-\ell_r)^2z_w\\&+(h_r-h_p)x_q]+\hat{m}\hat{g}h_r\ell_cx_u\}s+\hat{m}^2h_pf_{ce}\hat{m}\hat{g}=0\end{aligned} \tag{30}$$

Prior to the application of Routh's criteria to Eq. (30), it is useful to consider the signs of the three rotor derivatives. Reference 1 (p. 197) gives expressions for the rotor derivatives. In the earth-fixed axes, when $\theta_e=0$ the derivatives of interest for hovering flight in still air are

$$z_w=-2a\lambda_i/(16\lambda_i+as), \qquad x_q=(2a\lambda_i-16t_{ce})/\gamma,$$

$$x_u=-a/2\cdot(\delta/2a+8/9\cdot\theta_0^2-2\theta_0\lambda_i+\lambda_i^2), \text{ per rotor}$$

These three derivatives take negative values for all reasonable parameter sets. Consequently, it is assumed that the derivatives z_w, x_q and x_u are always negative.

Application of Routh's criteria to Eq. (30) yields seven inequalities, which must simultaneously be satisfied if the machine is to be stable. These seven conditions may be stated as

$$h_r(x_uh_r+x_q)<-(k^2+\ell_p^2)x_u-(\ell_p-\ell_r)^2z_w \tag{31}$$

$$0<h_p<(k^2+\ell_p^2)/\ell_c+(\ell_p-\ell_r)^2z_wx_u/\hat{m}f_{ce} \tag{32}$$

$$0<h_p<h_r\left[1+\frac{\ell_cx_u}{(\Gamma-1)(\ell_cx_u+x_q)}\right]+\frac{(\ell_p-\ell_r)^2z_w}{(\ell_cx_u+x_q)} \tag{33}$$

$$(\Gamma-1)>0 \tag{34}$$

$$\begin{aligned}0<\ell_c<[&\hat{m}f_{ce}((k^2+\ell_p^2+h_rh_p)^2x_u+h_p^2(\ell_p-\ell_r)^2z_w\\&+h_p(k^2+\ell_p^2+h_rh_p)x_q)]/\\&\div[(\hat{m}f_{ce}h_p-(\ell_p-\ell_r)^2z_wx_u)\cdot\Sigma\\&+\hat{m}(k^2+\ell_p^2)x_u(f_{ce}(h_r-h_p)+\hat{m}\hat{g}h_r)]\end{aligned} \tag{35}$$

$$\begin{aligned}&\hat{m}^2\hat{g}(\Gamma-1)^2[(k^2+\ell_p^2-h_p\ell_c)\Lambda\Sigma-(k^2+\ell_p^2)\Lambda^2]\\&+\ell_c(\Gamma-1)\{\hat{m}^2\hat{g}[(k^2+\ell_p^2-h_p\ell_c)h_rx_u\Sigma-h_p\Sigma^2\\&-2(k^2+\ell_p^2)h_rx_u\Lambda]+(\ell_p-\ell_r)^2z_wx_u\Sigma\Lambda\}\\&+\hat{m}\hat{g}\ell_ch_rx_u[\ell_c(\ell_p-\ell_r)^2z_wx_u\Sigma-\hat{m}\ell_c(k^2+\ell_p^2)h_rx_u]>0\end{aligned} \tag{36}$$

where

$$\Lambda=(h_r-h_p)(x_u\ell_c+x_q)+(\ell_p-\ell_r)^2z_w$$

$$\Sigma=(k^2+\ell_p^2+h_r^2)x_u+(\ell_p-\ell_r)^2z_w+h_rx_q$$

These inequalities define an envelope of stable configurations, which applies only to flat hovering flight on a vertical cable. They are subject to the limitations imposed by the assumptions $h_r\ll\ell_c$ and $h_p\ll\ell_c$ required to obtain Eqs. (33) and (36), and by the assumptions $h_r>0$ and $h_r>h_p$ made in obtaining Eq. (35). The latter two assumptions are made only to ensure that the denominator in Eq. (35) is positive. Although consistent with conventional rotorcraft practice, these assumptions may considerably restrict the generality of Eq. (35).

Even for the simple hovering case, the stability criteria are complicated. Essentially, they are implicit relationships which specify a maximum value of h_p, a maximum cable length, and a limiting thrust to weight ratio. These parameters were previously found to be important in the zero damping case. Again, static instability is predicted if h_p is negative. Inclusion of the rotor derivatives imposes a further geometrical restriction. Namely, Eq. (31) requires that h_r does not lie between two negative numbers. Since the stability boundaries implicit in Eqs. (31-36) are not obvious, it is instructive to consider some particular cases incorporating the rotor derivatives.

Stability with x_u and ℓ_c Small

A typical articulated rotor has derivatives x_u and x_q of the order of -0.05 and z_w of about -0.5. For rotors with heavy blades, such as those with counterweights or tip jets, the derivative x_q may be considerably larger than x_u. Since x_q is proportional to the reciprocal of the Lock number, γ, both z_w and x_q may be an order of magnitude greater than x_u. Under these circumstances, if x_u is neglected as being small, the Routh criteria become

$$h_rx_q<-(\ell_p-\ell_r)^2z_w, \qquad 0<h_p<(k^2+\ell_p^2)/\ell_c$$

$$0<h_p<h_p^*, \quad \text{where} \quad h_p^*=h_r+(\ell_p-\ell_r)^2z_w/x_q \tag{37}$$

$$0<\ell_c<\ell_c^*, \quad \text{where} \quad \ell_c^*=\frac{(k^2+\ell_p^2)x_q}{(\ell_p-\ell_r)^2z_w+h_rx_q} \tag{38}$$

$$\begin{aligned}(\Gamma-1)>\ell_c[(\ell_p-\ell_r)^2z_w+h_rx_q]^2/\{&\ell_c[(\ell_p-\ell_r)^2z_w+h_rx_q]\\&-(k^2+\ell_p^2)x_q\}[(\ell_p-\ell_r)^2z_w+(h_r-h_p)x_q\}\end{aligned}$$

The sole assumption inherent in these equations is that h_p/ℓ_c is small compared with unity. It is appropriate to neglect the derivative x_u in Eqs. (33) and (36) only if the cable is short. The term ℓ_cx_u in these equations indicates that x_u, the "drag

damping," becomes increasingly important at longer cable lengths.

Equations (37) and (38) define critical values of h_p and ℓ_c. Upon substitution of mh_p^* for h_p, and $n\ell_c^*$ for ℓ_c, all of the Routh criterion inequalities reduce to the single inequality

$$(\Gamma-1)>n/(1-n)(1-m); \qquad 0<m,n<1 \tag{39}$$

Equation (39) is graphed as Fig. 4. It can be seen that the minimum thrust to weight ratio required for stability becomes large as h_p approaches h_p^*, or as ℓ_c approaches ℓ_c^*. In practice, the thrust to weight ratio is unlikely to exceed three, and it is difficult to ensure that h_p is small and positive. With these considerations, Fig. 4 implies that practical cable lengths would be less than 40 percent of the critical value ℓ_c^*.

Stability on a Long Cable

When the cable length is large relative to the machine geometrical parameters, the stability quartic may be simplified by discarding some small terms. After multiplying Eq. (30) by $\epsilon=1/\ell_c$, the quartic becomes

$$[k^2+\ell_p^2]s^4-[(k^2+\ell_p^2+h_r^2)x_u+(\ell_p-\ell_r)^2z_w+h_rx_q]s^3$$
$$-[\hat{m}f_{ce}h_p-(\ell_p-\ell_r)^2z_wx_u]s^2-\hat{m}[f_{ce}(h_r-h_p)x_u$$
$$+\hat{m}\hat{g}h_rx_u]s+\epsilon\cdot\hat{m}^2\hat{m}\hat{g}f_{ce}h_p=0 \tag{40}$$

If ϵ or $h_p f_{ce}$ is zero, one power of s may be factored from the characteristic equation. Physically, when ϵ vanishes (i.e. $\ell_c=\infty$) an x-displacement of the cable attachment point produces no change in cable angle, and hence no component of cable force in the x-direction. This is equivalent to constraining the cable attachment point to translate in a horizontal frictionless slide. There is no stiffness in the x-direction, and the zero root represents the unconstrained translation along the "slide." Similarly, if $h_p f_{ce}$ is zero, a rotation engenders no change in pitching moment; there is no stiffness in the θ direction.

Since the cable length must be finite, the stability quartic will have one small real root, which will diminish in magnitude as ϵh_p decreases. Selection of a negative h_p leads to a small positive real root, representing a slow aperiodic divergence. After factorization of this small, approximately zero, root from the characteristic Eq. (40), the application of Routh's criteria to the remaining cubic gives the conditions for stability as

$$h_r(x_uh_r+x_q)<-(k^2+\ell_p^2)x_u-(\ell_p-\ell_r)^2z_w \tag{31}$$

$$h_p<(\ell_p-\ell_r)^2z_wx_u/\hat{m}f_{ce} \tag{41}$$

$$h_p<h_r\cdot\Gamma/(\Gamma-1) \tag{42}$$

$$[(k^2+\ell_p^2+h_r^2)x_u+(\ell_p-\ell_r)^2z_w+h_rx_q][\hat{m}h_pf_{ce}$$
$$-(\ell_p-\ell_r)^2z_wx_u]+\hat{m}(k^2+\ell_p^2)x_u(h_rt_{ce}-h_pf_{ce})>0$$

Recalling that all derivatives take negative signs, it can be seen that Eq. (31) is satisfied for any positive h_r. More specifically, this first condition is satisfied if

$$h_r>-[(k^2+\ell_p^2)x_u+(\ell_p-\ell_r)^2z_w]/x_q$$

or if

$$h_r<-x_q/x_u$$

These two limits are obtained from Eq. (31) as first terms of a truncated binomial series. When Eq. (41) is evaluated for typical parameters, the resulting upper value of h_p is a very small positive number. This value would not be greater than about 0.02% of the rotor radius when calculated at a thrust to weight ratio near 1.2. The requirement of Eq. (42) is easily satisfied. If h_p is positive, then Eq. (42) implies that h_r should also be positive. The inequality following may be rearranged to yield another limiting value of h_p. After discarding some small terms, this limit is approximately

$$h_p<-h_r\cdot\frac{\Gamma}{(\Gamma-1)}\,\frac{(k^2+\ell_p^2)x_u}{[(\ell_p-\ell_r)^2z_w+h_rx_q]} \tag{43}$$

In marked contrast to the previous short-cable result, the thrust to weight ratio does not strongly influence the stability of hovering flight on long cables. Previously, the limiting value of Γ resulted from a fourth-order Hurwitz determinant, whereas in the limit as $\epsilon\to 0$ Eq. (40) approaches a cubic form.

Solution of the Full Stability Quartic

A Fortran code has been developed to assemble and solve the complete stability quartic [Eq. (25)]. This code is applicable to tethered flight in wind or still air. The expressions used to evaluate the various rotor derivatives involve the assumption of small rotor disk incidences. The code has been used to generate numerical solutions to the full stability quartic for comparison with the analytic predictions of the Routh-Hurwitz stability criteria. It is important to note that Figs. 4-7 apply only to hovering flight in still air with $\theta_e=0$.

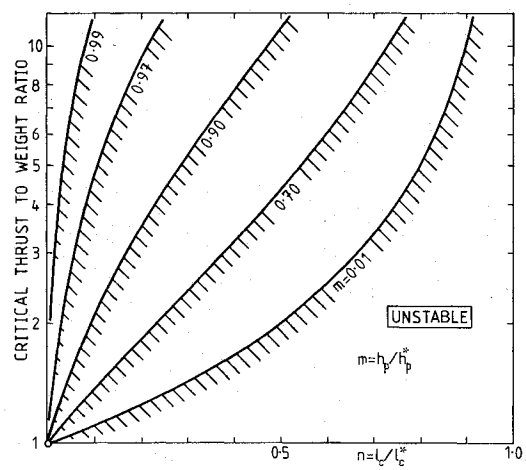

Fig. 4 Approximate stability boundaries on a short cable, with x_{ur} small.

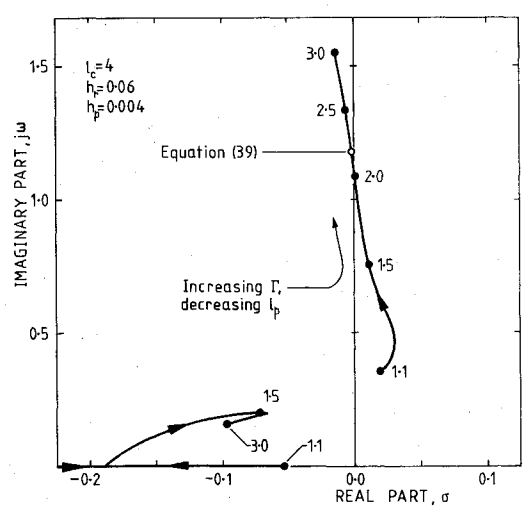

Fig. 5 Influence of thrust to weight ratio for a short tether cable.

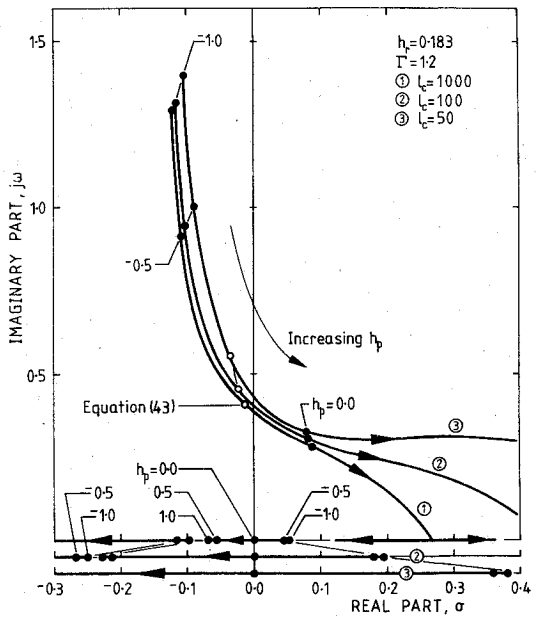

Fig. 6 Influence of attachment point height for long tether cables at sea level air density.

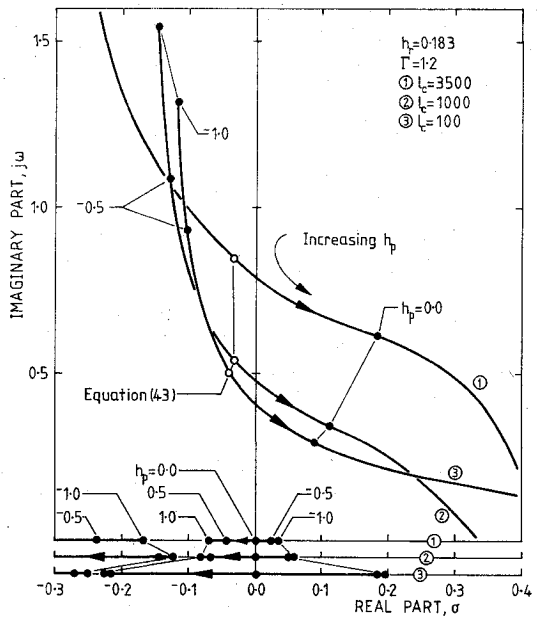

Fig. 7 Influence of attachment point height for long tether cables in US standard atmosphere.

Figure 5 shows the effect of thrust to weight ratio on the stability of an example machine restrained by a short vertical cable. Numerical values of parameters defining this example machine are given in Appendix 3. The figure demonstrates that inherent stability is possible if the operational thrust to weight ratio exceeds the critical value defined by Eq. (39), provided that both h_p and ℓ_c satisfy the restriction of Eqs. (37) and (38). It is important to appreciate that to preserve moment equilibrium with $\theta=0$, ℓ_p must decrease as Γ alone is increased. Furthermore, since the rotor derivatives depend on the thrust level, the critical values of h_p, ℓ_c and Γ all vary as the operational thrust to weight ratio changes. The predicted critical point is shown as an open circle in Fig. 5. The small real part of this root is due to the neglect of x_u in deriving Eq. (39).

When considering the stability of hovering flight on long cables, it is useful to know the cable length which is effectively "infinitely long." This length would then represent the lower bound of applicability of the long cable stability criteria of Eqs. (31) and (41-43). For certain fixed cable lengths, Fig. 6 shows loci of roots of the characteristic equation as h_p is varied. To demonstate the influence of cable length, the air density has artificially been fixed at a sea level value, regardless of the cable length. The loci of Fig. 6 consist of a complex pair representing oscillatory motion and two real roots which indicate aperiodic motion. As h_p increases from a negative value, the damped oscillation beomes divergent. The aperiodic divergence becomes convergent as h_p passes through zero to take positive values. With decreasing cable length, this aperiodic motion becomes increasingly rapid. When the cable is long, changes in ℓ_c have no appreciable effect on the oscillatory mode. However, if the cable length is small, further reductions in ℓ_c affect the damping and frequency of the oscillation. Figure 6 shows that for the example machine operating at $\Gamma=1.2$, the oscillatory motion is largely independent of cable length for ℓ_c greater than approximately 100.

The assumption that air density is constant is adequate at low altitudes but is not acceptable at altitudes above about one km. The decreased density at altitude significantly affects the oscillatory roots but has little influence on the aperiodic motion. In contrast to Fig. 6, Fig. 7 has been constructed assuming the air density varies according to the US standard atmosphere. Since the rotor derivatives x_q and m_q vary in inverse proportion to γ, these derivatives are sensitive to variations in air density. As is evident from a comparison of Fig. 6 and 7, a decrease in ρ increases both the frequency and damping ratio of the oscillatory motion. There is but slight effect on the aperiodic motion. The increase in frequency is futher compounded as the unit of dimensionless time becomes shorter with decreasing air density.

Conclusions

In preceding sections, linearized equations describing the longitudinal motion of a tethered rotorcraft about any equilibrium position have been derived. By using a straight-cable approximation, the equations are cast in the angular ordinates θ and α_c. The two degree-of-freedom equations do not require the assumption of constant cable tension.

The following conclusions may be drawn regarding the stability of a tethered rotorcraft, hovering in still air.

1) The cable length, equilibrium force, and point of attachment each strongly influence the machine's stability. These parameters are dominant even if all rotor damping is ignored. Static instability results from attaching the cable below the machine's center of gravity.

2) When the cable is short, i.e., $\ell_c<0(10)$, inherent stability may be attained by choosing h_p small and positive and operating at a high thrust to weight ratio. Upper bounds or critical values of h_p and ℓ_c exist and depend on the machine geometry and rotor parameters.

3) If the cable is long, i.e., $\ell_c>0(100)$, the machine configurations embodied in Figs. 1 and 2 appear to be unstable in flat hover for all rotor and tether attachment point locations. The system is characterized by an aperiodic divergence (static instability) if h_p is negative, and by oscillatory instability if h_p is greater than about -0.1. The aperiodic component of motion becomes slower as the magnitude of ϵh_p decreases. When $h_p=0$, there is no stiffness in the θ direction. If ϵ vanishes, the stiffness in the α_c direction is zero. Either condition implies the characteristic equation has a zero root.

4) At altitude, the reduced air density significantly affects the oscillatory roots, particularly if the blade Lock number is small.

Appendix 1

The various dimensionless lengths are

$$h_1 = \ell_p \sin\theta_e + h_p \cos\theta_e$$

$$\ell_1 = \ell_p \cos\theta_e - h_p \sin\theta_e$$

$$h_2 = \ell_p \cos(\alpha_{ce} + \theta_e) - h_p \sin(\alpha_{ce} + \theta_e)$$

$$\ell_2 = \ell_p \sin(\alpha_{ce} + \theta_e) + h_p \cos(\alpha_{ce} + \theta_e)$$

$$h_3 = \ell_r \sin\theta_e + h_r \cos\theta_e$$

$$\ell_3 = \ell_r \cos\theta_e - h_r \sin\theta_e$$

$$h_4 = -\ell_t \sin\theta_e + h_t \cos\theta_e$$

$$\ell_4 = \ell_t \cos\theta_e + h_t \sin\theta_e$$

Appendix 2

In enumerating lift and drag effects, the tailplane derivatives allow for the downwash induced by the rotor at the tailplane. It is assumed that the steady state downwash at the tail is of uniform magnitude kv_{i0}, and is parallel to the TPP axis. The factor k is a multiplier of the "uniform" velocity induced at the rotor, v_{i0}. Momentum theory applied to the wake indicates $k=1$ at the rotor, and $k=2$ in the fully developed wake. For other positions, k could be estimated from the data of Heyson and Katsoff,[18] for example. For a twin rotor machine, interference effects may also be significant. The expressions for the downwash lag derivatives $m'_{ut}rom'_{wt}$, and m'_{qt} are valid only for flight in wind at μ greater than about 0.1. In hover, these derivatives tend to zero as the rotor induces little flow at the tailplane: i.e., $k \approx 0$.

With these assumptions, the tailplane derivatives are

$$x_{nt} = \hat{A}[K_1 D_n + K_2 G_n], \qquad n = \acute{u}, \acute{w}, \acute{q}, u, w, q$$

$$x_{\theta t} = \hat{A}[K_1 D_\theta + K_2 G_\theta + K_3]$$

$$x_\zeta = \hat{A} \cdot K_3$$

$$z_{nt} = \hat{A}[K_4 D_n + K_5 G_n], \qquad n = \acute{u}, \acute{w}, \acute{q}, u, w, q$$

$$z_{\theta t} = \hat{A}[K_4 D_\theta + K_5 G_\theta + K_6]$$

$$z_\zeta = \hat{A} \cdot K_6$$

$$m_{nt} = x_{nt} h_4 - z_{nt} \ell_4, \qquad n = \acute{u}, \acute{w}, \acute{q}, u, w, q, \zeta$$

$$m_{\theta t} = x_{\theta t} h_4 - z_{\theta t} \ell_4 + \hat{L}_e h_4 - \hat{D}_e \ell_4$$

where

$$K_1 = C_d \hat{U}_x - C_\ell \hat{U}_z \qquad K_3 = \tfrac{1}{2}[d \cdot \hat{U}_x - e \cdot \hat{U}_z]\hat{U}$$

$$K_2 = \tfrac{1}{2}[(d - C_\ell)\hat{U}_x - (e + C_d)\hat{U}_z] \qquad K_4 = C_\ell \hat{U}_x \times C_d \hat{U}_z$$

$$K_5 = \tfrac{1}{2}[(e + C_d)\hat{U}_x + (d - C_\ell)\hat{U}_z] \qquad K_6 = \tfrac{1}{2}[e \cdot \hat{U}_x + d \cdot \hat{U}_z]\hat{U}$$

$$d = \epsilon_1 \cos\alpha_r - \epsilon_2 \sin\alpha_r \qquad e = a_t \cos\alpha_r$$

$$\hat{A} = A_t / s A_r$$

$$\partial \hat{U}_x / \partial \acute{n} \approx k\Delta\tau[S \cdot \partial\lambda_i/\partial n + \lambda_i C \cdot \partial a_1/\partial n], \quad n = \hat{u}, \hat{w}, \hat{q}$$

$$D_n = \left(\frac{\hat{U}_x}{\hat{U}} \cdot \frac{\partial \hat{U}_x}{\partial n} + \frac{\hat{U}_z}{\hat{U}} \cdot \frac{\partial \hat{U}_z}{\partial n}\right), \qquad n = \acute{\hat{u}}, \acute{\hat{w}}, \acute{\hat{q}}, \hat{u}, \hat{w}, \hat{q}, \theta$$

$$G_n = \left(\frac{\hat{U}_x}{\hat{U}} \cdot \frac{\partial \hat{U}_z}{\partial n} - \frac{\hat{U}_z}{\hat{U}} \cdot \frac{\partial \hat{U}_x}{\partial n}\right), \qquad n = \acute{\hat{u}}, \acute{\hat{w}}, \acute{\hat{q}}, \hat{u}, \hat{w}, \hat{q}, \theta$$

In the above equations,

$$\hat{U}_x = \hat{U}_0 - k\lambda_i S \qquad \hat{U}_0 = U_0/\Omega R$$

$$\hat{U}_z = -k\lambda_i C \qquad \lambda_i = v_{i0}/\Omega R$$

$$\hat{U}^2 = \hat{U}_x^2 + \hat{U}_z^2$$

The derivatives are

$$\partial \hat{U}_x/\partial \hat{u} = -[kS \cdot \partial\lambda_i/\partial \hat{u} + k\lambda_i C \cdot \partial a_1/\partial \hat{u} + 1]$$

$$\partial \hat{U}_z/\partial \hat{u} = -[kC \cdot \partial\lambda_i/\partial \hat{u} - k\lambda_i S \cdot \partial a_1/\partial \hat{u}]$$

$$\partial \hat{U}_x/\partial \hat{w} = -[kS \cdot \partial\lambda_i/\partial \hat{w} + k\lambda_i C \cdot \partial a_1/\partial \hat{w}]$$

$$\partial \hat{U}_z/\partial \hat{w} = -[kC \cdot \partial\lambda_i/\partial \hat{w} - k\lambda_i S \cdot \partial a_1/\partial \hat{w} + 1]$$

$$\partial \hat{U}_x/\partial \hat{q} \approx -h_4 - k\lambda_i C \cdot \partial a_1/\partial \hat{q} + k\Delta\tau[\lambda_i C(1 + \partial a_1/\partial\theta) + S \cdot \partial\lambda_i/\partial\theta]$$

$$\partial \hat{U}_z/\partial \hat{q} \approx \ell_4 + k\lambda_i S \cdot \partial a_1/\partial \hat{q} - k\Delta\tau[\lambda_i S(1 + \partial a_1/\partial\theta) - C \cdot \partial\lambda_i/\partial\theta]$$

$$\partial \hat{U}_x/\partial\theta = -kS \cdot \partial\lambda_i/\partial\theta - k\lambda_i C[1 + \partial a_1/\partial\theta]$$

$$\partial \hat{U}_z/\partial\theta = -kC \cdot \partial\lambda_i/\partial\theta + k\lambda_i S[1 + \partial a_1/\partial\theta]$$

$$\partial \hat{U}_x/\partial \acute{n} \approx k\Delta\tau[S \cdot \partial\lambda_i/\partial n + \lambda_i C \cdot \partial_1 \cdot \partial a_1/\partial n], \quad n = \hat{u}, \hat{w}, \hat{q}$$

$$\partial \hat{U}_z/\partial \acute{n} \approx k\Delta\tau[C \cdot \partial\lambda_i/\partial n - \lambda_i S \cdot \partial a_1/\partial n], \quad n = \hat{u}, \hat{w}, \hat{q}$$

where

$$S = \sin(\theta_e + a_{1e}) \qquad C = \cos(\theta_e + a_{1e})$$

$$\alpha_r = \theta + \zeta + \phi \qquad \phi = \tan^{-1}(\hat{U}_z/\hat{U}_x)$$

$$\Delta\tau \approx (\ell_3 + \ell_4)/\hat{m}\hat{U}_0$$

Appendix 3

Numerical values used to construct Figs. 5-7 are

$a = 5.200\ \text{rad}^{-1}$	$\ell_r = 0.0600$
$B = 2.853\ \text{kg-m}^2$	$m = 30.00\ \text{kg}$
$b = 1$	$R = 1.803\ \text{m}$
$c = 0.1240\ \text{m}$	$\delta = 0.012$
$k^2 = 0.4730$	$\Omega = 62.83\ \text{rad s}^{-1}$

Acknowledgment

The writer wishes to thank the members of the gyromill group at the University of Sydney, especially Associate Professor B.W. Roberts, for much helpful discussion.

References

[1]Bramwell, A.R.S., *Helicopter Dynamics,* 1st ed., Arnold, London, 1976, pp. 191-193.

[2]Liptrot, R.N., "Rotating Wing Activities in Germany During the Period 1939-1945," British Intelligence Objectives Sub-Committee. Overall Rept. 8, His Majesty's Stationery Office, London, 1948.

[3]McNeill, L.H., Plaks, A., and Blackburn, W.E., "Analysis of Unmanned, Tethered, Rotary-Wing Platforms," USAAMRDL TR-74-56, July 1974.

[4]Reigler, G., Riedler, W., and Horvath, E., "A Feasibility Study for High-Altitude Wind Power Plants," *Proceedings of the SERI 2nd*

Wind Energy Innovation Systems Conference, SERI CP-635-938, Solar Energy Research Institute, Vol. 1, Dec. 1980, pp. 94-111.

[5]Fletcher, C.A.J., and Roberts, B.W., "Electricity Generation from Jet-Stream Winds," *Journal of Energy,* Vol. 3, Jul.-Aug. 1979, pp. 241-249.

[6]Roberts, B.W., and Blackler, J., "Various Systems for the Generation of Electricity Using Upper Atmospheric Winds," *Proceedings of the SERI 2nd Wind Energy Innovation Systems Conference,* SERI CP-635-938, Solar Energy Research Institute, Vol. 1, Dec. 1980, pp. 68-90.

[7]Noll, R.B., and Ham, W.D., "Tethered Gyroturbine Wind Energy System," *Proceedings of the SERI 2nd Wind Energy Innovation Systems Conference,* SERI CP-635-938, Solar Energy Reserach Institute, Vol. II, Dec. 1980, pp. 19-26.

[8]Blackler, J., Nibbe, H., Barratt, A.J., and Roberts, B.W., "Experiments with a Twin Rotor Gyromill," Solar Energy at Work Conference, International Solar Energy Society (A.N.Z.), Sydney, Nov. 1981.

[9]Kaufman, L., and Schultz, E.R., "The Stability and Control of Tethered Helicopters," *Journal of the American Helicopter Society,* Vol. 7, Oct. 1962, pp. 41-54.

[10]Schmidt, G., and Swik, R., "Theoretical and Practical Aspects of an Automatic Hover Control System for an Unmanned Tethered Rotorcraft," *Proceedings of the 5th World Congress,* International Federation of Automatic Control, Part II, Düsseldorf, German Federal Republic, June 1972, pp. 19.11-19.18.

[11]Rye, D.C., Blackler, J., and Roberts, B.W., "The Stability of a Tethered Gyromill," AIAA Paper 81-2569, Dec. 1981.

[12]Glauert, H., "The Stability of a Body Towed by a Light Wire," Aeronautical Research Committee, R.&M. 1312, His Majesty's Stationery Office, London, Feb. 1930.

[13]Huffman, R.R. and Genin, J., "The Dynamical Behaviour of a Flexible Cable in a Uniform Flowfield," *Aeronautical Quarterly,* Vol. XXII, May 1971, pp. 183-195.

[14]Phillips, W.H., "Theoretical Analysis of Oscillations of a Towed Cable," NACA TN 1796, Jan. 1949.

[15]DeLaurier, J.D., "A First Order Theory for Predicting the Stability of Cable Towed and Tethered Bodies Where the Cable Has a General Curvature and Tension Variation," von Kármán Institute for Fluid Dynamics, Rhode-Saint-Genese, Belgium, VKI TN 68, Dec. 1970.

[16]Castles, W. Jr. and New, N.C., "A Blade Element Analysis for Lifting Rotors that is Applicable for Large Inflow and Blade Angles and Any Reasonable Geometry," NACA TN 2656, July 1952.

[17]Nissim, E., "On a Specialized Case of the Routh-Hurwitz Stability Criteria," *Aeronautical Quarterly,* Vol. XIX, Nov. 1968, pp. 352-356.

[18]Heyson, H.H., and Katzoff, S., "Induced Velocities Near a Lifting Rotor with Nonuniform Disk Loading," NACA Report 1319, 1957.